Journal of Organometallic Chemistry 694 (2009) 1795–1801

Contents lists available at ScienceDirect

Journal of Organometallic Chemistry

journal homepage: www.elsevier.com/locate/jorganchem

Mono and bimetallic nickel bromide complexes bearing azolate-imine ligands: Synthesis, structural characterization and ethylene polymerization studies

Rodrigo Caris [a], Brian C. Peoples [b], Mauricio Valderrama [a], Guang Wu [c], Rene Rojas [a,b,*]

[a] Departamento de Química Inorgánica, Facultad de Química, Pontificia Universidad Católica de Chile, Casilla 306, Santiago-22, Chile
[b] Centro para la Investigación Interdisciplinaria Avanzada en Ciencias de Materiales (CIMAT), Chile
[c] Departments of Chemistry and Materials, University of California, Santa Barbara, CA 93106, United States

ARTICLE INFO

Article history:
Received 13 November 2008
Received in revised form 7 January 2009
Accepted 8 January 2009
Available online 14 January 2009

Keywords:
Nickel
Azolate-imine ligands
Ethylene polymerization
Branching PE
Late transition metal catalysts

ABSTRACT

The synthesis of *N*-(1-(3,5-dimethylpyrazol-1-yl)ethylidene)-2,6-diisopropylaniline (**1**) and *N*-(1-(indazol-2-yl)ethylidene)-2,6-diisopropylaniline (**2**) allowed access to new transition metal complexes. When reacted with dibromo(2,2′-dimethoxyethylether)nickel(II) the complexes [$NiBr_2${*N*-(1-(3,5-dimethylpyrazol-1-yl)ethylidene)-2,6-diisopropylaniline}] (**3**) and [$Ni_2Br_2(\mu\text{-}Br)_2${*N*-(1-(indazol-1-yl)ethylidene)-2,6-diisopropylaniline}$_2$] (**4**) are yielded, respectively. The addition of MAO generates catalytically active species for the homopolymerization of ethylene. The polymer products were low molecular weight (3–6 K) and a monomodal molecular weight distribution, consistent with the presence of a single active site. In addition, the catalyst was found to efficiently oligomerize higher olefins to high molecular weights with narrow PDIs.

1. Introduction

Synthetic control and tailoring of bulk polyolefin properties is a major focus of many industrial and academic research groups. Advances in the design of single site catalysts provide an ever-increasing array of metal–ligand combinations suitable for catalyzing the polymerization of olefins [1–6]. A substantial body of mechanistic work exists which provides insight into how the active site structure influences the polymerization process. General trends have emerged in the design of catalyst structure, which allow for the production of a specific polymer microstructure and also of important bulk properties of the resulting polymer through catalyst design. Single site catalyst systems have made a considerable impact on the commercial processes that produce these commodity products [7,8]. While polyolefin research initially focused on early transition metals, such as zirconium and titanium, there has been a shift over the last 20 years to an increased emphasis on the late transition metals such as iron, nickel and palladium [9–19]. This shift is based largely on the reduced oxophilicity of the late transition metals and the ease with which large ligand libraries and catalysts can be generated. With the late transition metal system it was not only feasible to prepare known polyolefinic materials under gentle conditions (i.e. low pressure and temperature), but also new materials with well defined molecular characteristics, including a variety of functionalities [20–27]. A majority of these late transition metal complexes are based on bi, tri and tetra dentate organic molecules coordinated to a metal center. These systems are based on catalytic oligomerization (a major industrial process) [27–29] processes, in which Ni or Pd metal centers chelated by PN or PP ligands are used [30–33]. It was realized that the size and structure of the ligands could change the product distribution of the process to produce higher molecular weight polymers. The bonding versatility and the relative ease with which the electronic and steric properties of the P and N atoms can be modified make them attractive as the basis for these ligands. In theory, the reactivity, selectivity and the ability to oligomerize or polymerize monomers is defined by the electronic, steric and geometric (chelate ring size) effects of the ligand. In the case of N,N or N,O bidentate ligands [34–37], the size of the aromatic substituents on the imine or imide and carboxamide nitrogens would influence ligand coordination mode (i.e., N,N versus N,O) [38–40], the reactivity and the propagation and termination ratio, allowing access to a variety of new materials.

Considerable efforts have been focused on understanding the role of co-activators on mediating these polymerization processes [41]. Zwitterionic complexes, where a partial positive charge formally resides at the metal center, constitute a smaller class of initiators [42–51]. In many instances, Lewis acids are used to activate the metal center upon coordination to a basic functionality on the ligand framework at a site removed from the metal center [52–56]. This type of activation places the Lewis acid away from

* Corresponding author. Address: Departamento de Química Inorgánica, Facultad de Química, Pontificia Universidad Católica de Chile, Casilla 306, Santiago-22, Chile. Tel.: +56 2 3547557; fax: +56 2 3544744.
E-mail address: rrojasg@uc.cl (R. Rojas).

0022-328X/$ - see front matter © 2009 Elsevier B.V. All rights reserved.
doi:10.1016/j.jorganchem.2009.01.005

the trajectory of monomer insertion and eliminates the complexities associated with the use of alkylaluminoxanes in which anion de-coordination or displacement is required for monomer insertion [57]. Bidentate or tridentate ligand frameworks which have additional peripheral heteroaromatic subtituents have been reported, in particular *N*-hetaryl 1,2-diimine or *N*,*N*,*N*-bis(imino)pyridine ligands [35,58]. These types of ligands were reported to easily complex the appropriate transition metal halide but the influence of the heteroaromatic substituent on the reactivity and polymers properties was not discussed.

In an effort to better understand the effects of heteroaromatic substituents on the reactivity and polymer properties, the synthesis of *N*-(1-(3,5-dimethylpyrazol-1-yl)ethylidene)-2,6-diisopropylaniline and *N*-(1-(indazol-2-yl)ethylidene)-2,6-diisopropylaniline ligands and subsequent metalation by nickel dibromide complexes was pursued. During the preparation of this manuscript, similar ligands and complexes where reported by Wu and co-workers [59]. The activity of such complexes and their catalytic behavior is described along with the characterization of the products.

2. Results and discussion

The ligands *N*-(1-(3,5-dimethylpyrazol-1-yl)ethylidene)-2,6-diisopropylaniline (**1**) and *N*-(1-(indazol-2-yl)ethylidene)-2,6-diisopropylaniline (**2**) were synthesized by reacting imidoyl chloride [60] with a 10% excess of 3,5-dimethylpyrazole or indazole in presence of Et_3N in toluene at reflux. This reaction path yields ligands **1** and **2**, respectively, (Eq. (1) and Scheme 1).

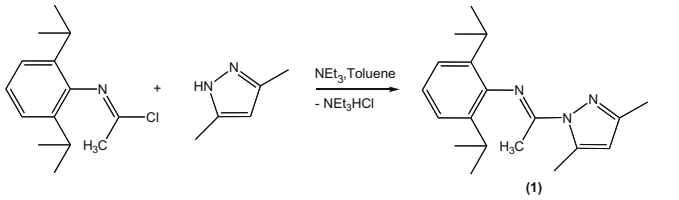

(1)

To isolate compound **1**, after 24 h refluxing in toluene the suspension was filtered and the solvent was removed providing light brown oil in 89% yield. The ^1H and ^{13}C NMR spectra are consistent with the formation of a single isomer of compound **1**. Diagnostic peaks include (in ppm): 6.01 (s, 1H, *H*-3,5-Me_2Pz) 2.8–2.9, (hept, 2H, *CH*-*i*Pr), 2.66 (s, 3H, CH_3), 2.29 (s, 3H, *Me*-Pz) and 2.28 (s, 3H, *Me*-Pz).

The addition of imidoyl chloride to indazol can result in the formation of two isomers. While both are isolable, an effort was made to isolate **2** rather than **2′** as this isomer is more desired as it maintains the geometry produced in **1**. Compound **2** was isolated by filtering the suspension and removing the solvent to provide a crude white powder. As shown in Scheme 1, the nature of the base defines the regiochemistry of the reaction. When a depronating base is used it is thought that two regioisomers can be obtained from this reaction; the N-1(**2′**) and N-2(**2**) substituted indazoles, (Scheme 1, right). The reaction can be directed to the desired isomer **2**, depending on the base used [61]. In this particular case, using non-deprotonating bases such as NEt_3, the synthesis is directed towards the formation of isomer **2** only, since the electron pair at N-2 becomes more reactive than the corresponding one on N-1, which forms part of the aromatic system. It is also possible that the electron pair at N-2 facilitates the nucleophilic reaction over the imine carbon on the imidoyl chloride.

The pure product was isolated by recrystallization from methanol, and obtained as white crystals in 64% yield. The ^1H and ^{13}C NMR spectra are consistent with the formation of a single isomer. Diagnostic peaks include 2.82 (hept, 2H, *CH*-*i*Pr), 2.48 (s, 3H, CH_3) and 1.15 (d, 12H, CH_3-*i*Pr). The synthesis of [$NiBr_2${*N*-(1-(3,5-dimethylpyrazol-1-yl)ethylidene)-2,6-diisopropylaniline}] (**3**) by the addition of *N*-(1-(3,5-dimethylpyrazol-1-yl)ethylidene)-2,6-diisopropylaniline (**1**) to [$NiBr_2${$O(C_2H_4OMe)_2$}] in THF at room temperature is depicted in Eq. (2). Crystallization from dichloromethane-ether allows isolation of **3** as air and thermally stable dark purple crystals in 95% yield.

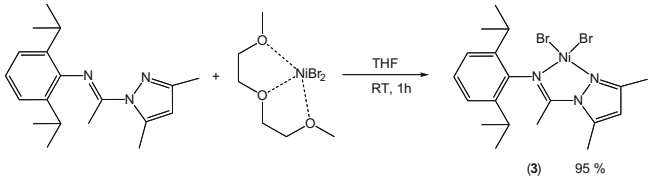

(2)

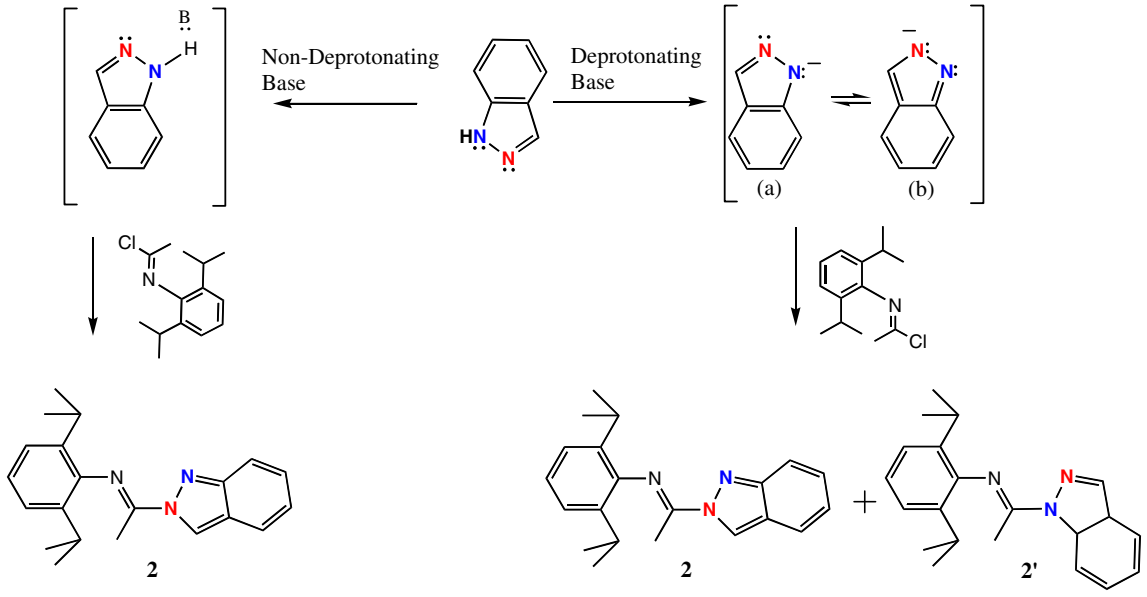

Scheme 1. Reaction of imidoyl chloride over indazol in the presence of depronating bases (i.e. NaH) and non-deprotonating bases (i.e. NEt_3).

Single crystals of **3** suitable for X-ray diffraction studies were obtained by diffusion of pentane into a toluene solution of the compound at room temperature. The results of these studies are shown in Fig. 1 and the crystallographic parameters in Table 1. The molecular structure, shows an *N*,*N*-binding mode for the *N*-(1-(3,5-dimethylpyrazol-1-yl)ethylidene)-2,6-diisopropylaniline and two bromides coordinated to the nickel. The tetrahedral geometry around nickel is distorted: for example, the angle N(1)–Ni–Br(1) (135.43 (5)°) is 34.61° longer than N(1)–Ni–Br(2) (100.82(5)°). Additionally as depicted in Fig. 1, the Br(1) atom is nearly perpendicular to the plane containing the five membered chelate ring.

The Ni–N(1), Ni–N(3), Ni–Br(1) and Ni–Br(2) bond distances are 2.0113(16), 1.9618(18), 2.3251(4) and 2.3590(4), respectively. The N(1)–C(13), N(2)–C(13) and N(3)–N(2) bond distances of 1.280(3), 1.402(3) and 1.380(3), respectively, which are consistent with same degree of conjugation in the chelate ring through the pyrazol. The N(3)–C(17) and N(2)–C(15) bond distances are 1.330(3) and 1.383(3), respectively, which are similar to those of the chelate ring. The plane of the chelate ring is extended through the pyrazole fragment while the 2,6-*i*Pr phenyl fragment is perpendicular to the rest of the molecule, Fig. 1.

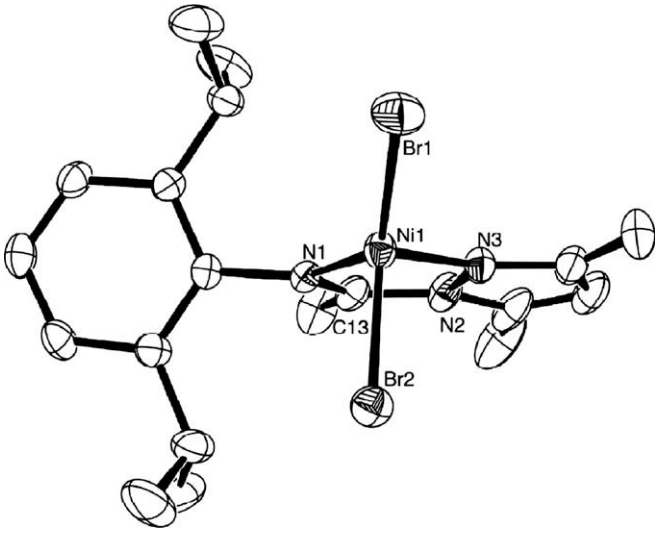

Fig. 1. ORTEP drawing of **3**, at 50% probability. Hydrogen atoms are omitted for clarity.

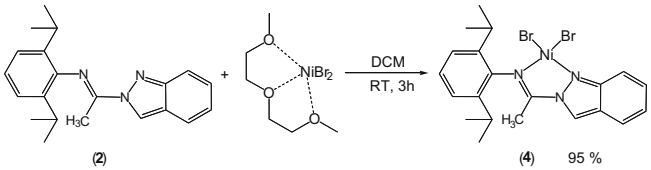

(3)

The synthesis of [$NiBr_2${*N*-(1-(indazol-1-yl)ethylidene)-2,6-diisopropylaniline}] (**4**) was carried out following the same procedure of compound **3**. Adding equimolar amounts of *N*-(1-(indazol-2-yl)ethylidene)-2,6-diisopropylaniline (**2**) to [$NiBr_2${($O(C_2H_4O\text{-}Me)_2$}] in dichloromethane at room temperature results in the formation of **4**, which was purified via crystallization from a pentane/diethyl ether mixture. Orange crystals were isolated in 80% yield (Eq. (3)).

The ^{1}H NMR spectrum of the product did not provide sufficient information to elucidate the purity of the reaction yield as **3** and **4** produce broad NMR signals which are associated with the paramagnetic nature of the tetrahedral geometry of these compounds. Single crystals of **4**, however, were easily obtained from an ether/pentane mixture and the resulting molecular structure is shown in Fig. 2 and the crystallographic parameters in Table 1.

The most significant feature of this structure is an unexpected bimetallic ligand arrangement around the two nickel centers, (dimer) without a central inversion center. The two molecules of **4** are bridged by two bromine atoms, leaving an unshared bromide ligand at each five-coordinate Ni center, resulting in a shared square pyramidal geometry with the apex of the pyramid oriented in the same direction while the Ni centers, ligand framework and

Table 1
Selected bond lengths (Å) and bond angles (°) of complexes **3** and **4**.

3		**4**	
Bond distances			
Ni–Br(1)	2.3251(4)	Ni(1)–Br(1)	2.4831(16)
Ni–Br(2)	2.3590(4)	Ni(1)–Br(2)	2.4335(16)
Ni–N(1)	2.0113(16)	Ni(1)–N(1)	2.065(7)
Ni–N(3)	1.9618(18)	Ni(1)–N(3)	2.025(6)
N(3)–N(2)	1.380(3)	N(2)–N(3)	1.341(10)
N(2)–C(13)	1.402(3)	N(1)–C(1)	1.248(9)
N(1)–C(13)	1.280(3)	N(2)–C(1)	1.421(11)
N(1)–C(1)	1.451(3)	N(2)–C(3)	1.361(10)
N(2)–C(15)	1.383(3)	N(3)–C(9)	1.382(9)
N(3)–C(17)	1.330(3)	N(1)–C(10)	1.525(11)
Bond angles			
Br(1)–Ni–Br(2)	113.536(14)	Br(1)–Ni–Br(1)*	86.26(5)
N(3)–Ni–N(1)	80.04(7)	N(3)–Ni–N(1)	77.4(3)
N(3)–Ni–Br(1)	115.46(6)	N(3)–Ni–Br(1)	96.1(29)
N(1)–Ni–Br(1)	135.43(5)	N(1)–Ni–Br(1)	154.6(2)
N(3)–Ni–Br(2)	104.52(5)	Br(1)*–Ni–N(1)	94.16(18)
N(1)–Ni–Br(2)	100.82(5)	Br(1)*–Ni–Br(2)	102.44(6)
N(2)–N(3)–Ni	112.69(13)	N(1)–Ni–Br(2)	154.6(2)
N(1)–C(13)–N(2)	115.28(19)	N(3)–Ni–Br(2)	91.0(2)
C(13)–N(1)–C(1)	120.01(17)	Br(1)–Ni–Br(2)	107.96(6)
C(13)–N(1)–Ni	115.53(14)	Ni–Br(1)–Ni*	92.58(5)
N(3)–N(2)–C(15)	110.1(2)	N(2)–N(3)–Ni	110.0(5)
N(3)–N(2)–C(13)	115.89(17)	Ni–N(1)–C(1)	115.8(6)
C(17)–N(3)–N(2)	106.44(19)	N(1)–C(1)–N(2)	113.6(8)
		C(1)–N(2)–N(3)	118.2(7)

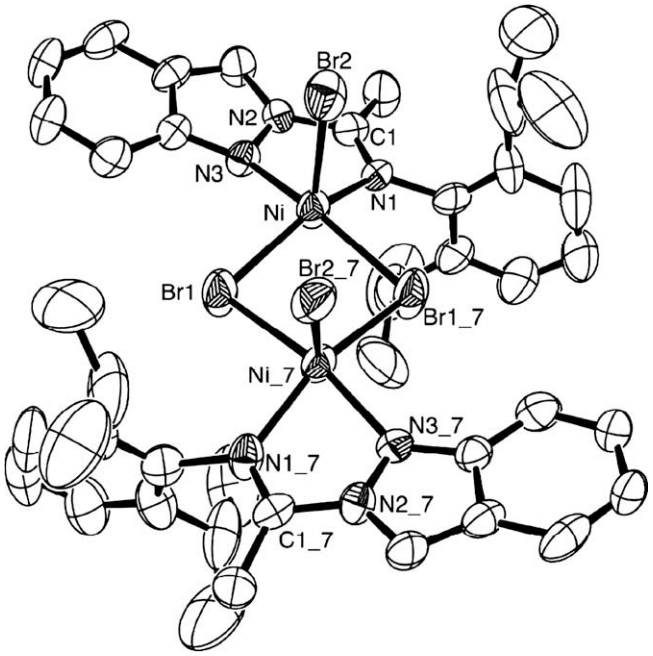

Fig. 2. ORTEP drawing of **4**, drawn at 50% probability. Hydrogen atoms were omitted for clarity.

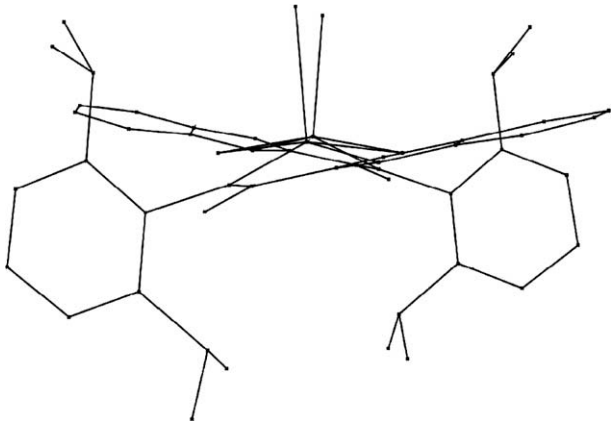

Fig. 3. Stick ORTEP drawing of **4**.

two of the bromides occupying, for intensive purposes, a shared plane. As can be seen in Fig. 3, the ligands are not coplanar but rather assume a gauche configuration. This distortion relieves steric crowding and separates the two *i*Pr groups from the indazol ring.

Table 2
Ethylene polymerization reactions.[a]

Entry	Precatalyst[a] (μmol)	Time[b]	*T* (°C)	*P*[c]	Yield[d]	*A*[e]	M_w	PDI
1	**3** (9.6)	10	20	100	0.7	435	6500	1.9
2	**3** (9.6)	10	40	100	1.3	807	3600	2.2
3	**4** (7.8)	10	20	100	2.8	2231	2750	2.0
4	**4** (7.8)	10	40	100	3.8	2890	1900	1.9
5	**4** (2.2)	10	20	300	2.9	7634	4000	2.0
6	**4** (2.2)	20	20	300	5.8	7400	5000	1.6
7	**4** (2.2)	40	20	300	12.0	8000	4300	1.7

[a] Polymerizations were carried out in 100 mL autoclave reactors in 30 mL toluene at 20 °C, the internal temperature was measured by using a thermocouple and was controlled using an external cooling bath, ratio Al/Ni, 1000.
[b] Time in minutes.
[c] Ethylene pressure in psi.
[d] Grams.
[e] Activity in g polymer/(mmol Ni) (h).

The bond distances in the X-ray structure of **4** reveal interesting bond characteristics. As the framework of the ligand is planar we suspected that there would be substantial overlap of the p orbitals and that conjugation along the ligand framework (through the indazole ring and including the imine) would be observed. The length of N(1)–C(1), C(1)–N(2) and N(3)–N(2) bond distances in the chelate ring, 1.248(9), 1.421(11) and 1.341(10), respectively, indicate however that the conjugation is not extended over the chelate ring. The bond distances in the indazole ring, N(2)–C(3) and N(3)–C(9) measuring 1.361(10) and 1.382(9) Å, are indicative of conjugation. Similar distances are observed in **3** as well.

Studies of the homopolymerization of ethylene using compounds **3** and **4** activated with methylaluminoxane (MAO) were carried out and the results are summarized in Table 2. These polymerization reactions were performed in a 100 mL autoclave reactor in 30 mL of toluene. Entries 1 and 2 show the results obtained at 20 and 40 °C reaction temperature with compound **3**/MAO. Comparison of these entries shows that while the ethylene consumption is higher at 40 °C. The molecular weights of the polymers decrease with higher polymerization temperatures. The PDIs (Mw/Mn ratio) are approximately 2, slightly narrower than that of the polyethylene obtained at 20 °C. Entries 3–7 show the results obtain with compounds **4**/MAO at different reaction condition and demonstrate that these combinations also yield ethylene polymerization sites. Analysis of the polymerization solutions by GC–MS did not reveal the presence of ethylene dimers, trimers or tetramers.

A comparison of entries 3, and 4, with 1 and 2, respectively, under similar reaction conditions show that the polymerization activity is higher with **4**/MAO systems. However, there is a decrease in the molecular weight of the polyethylene product probably associated with the reduction of the steric bulk on the ligand, particularly in the proximity of the nickel center; interestingly the PDIs do not change. Additionally for **4**/MAO systems there was a change in the ethylene consumption rate when the ethylene pressure was varied between 100 and 300 psi. Entries 3 and 5 show that an increase in the ethylene pressure provides higher activity, and results in high molecular weight products without increases to the PDI. Entries 5–7 show the results obtained at different reaction times with **4**/MAO systems. Comparison of these entries shows that the yield of the reaction increases proportionally over time, but the molecular weight remains fairly constant. The PDIs

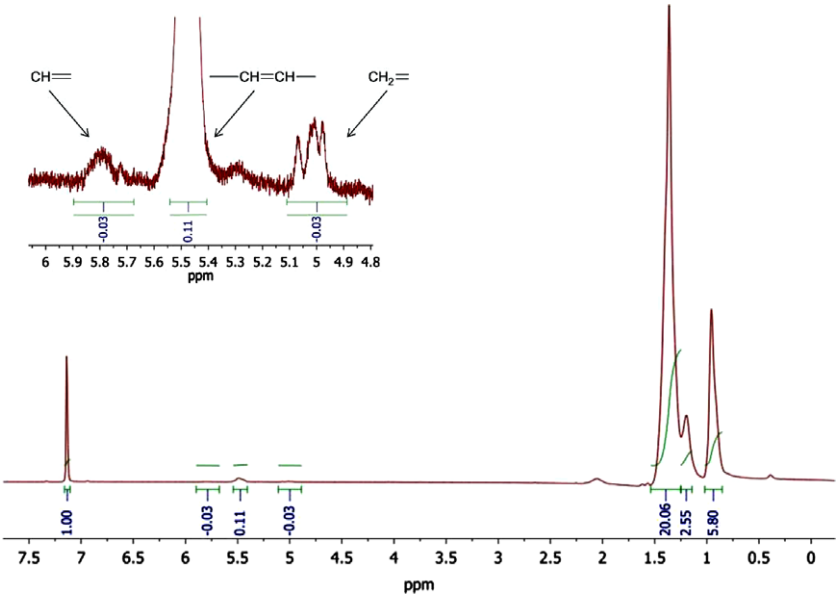

Fig. 4. ^{1}H NMR spectra of product (Entry 4, Table 1).

Table 3
1-Decene polymerization reactions.[a]

Entry	Precatalyst[a] (μmol)	Time[b]	T (°C)	Yield[c]	Conversion[d] (%)	M_w	PDI
1	**4** (10.8)	60	20	–	–	–	–
2	**4** (10.8)	60	40	0.55	11	2027	1.03
3	**4** (10.8)	60	60	0.60	24	2209	1.05
4[e]	**4** (10.8)	60	40	0.50	10	<500	–

[a] Polymerizations were carried out in Schlenk tubes in 15 g toluene at the temperature indicated. The internal temperature was maintained by an external water bath. A solution of the catalyst, 10.8 μmol in 5 g toluene, was injected through a rubber septa into a Schlenk tube containing a solution of 1-decene (5 g) in 10 g toluene and 0.035 mg of MAO, ratio Al/Ni, 30.
[b] Time in minutes.
[c] Grams.
[d] Conversion = grams isolated product/grams monomer injected.
[e] 1 g MAO solution was used, ratio Al/Ni 860.

(Mw/Mn ratios) of the polyethylene obtained are more narrow (1.6 and 1.7) for longer reaction times than for those with shorter durations (2.0).

The products obtained from polymerizations with **3** and **4**/MAO were surprisingly not solids, but rather waxy materials, which in our experience is an indication of highly branched materials. In order to elucidate the polymer structure the materials were analyzed by ^{1}H NMR and ^{13}C NMR techniques. Fig. 4 shows the ^{1}H NMR while the ^{13}C NMR spectra is available in the supplementary information.

Of particular interest is the peaks assigned to internal olefins at δ 5.5 ppm. The integration of the peak, is ca. 3.6 times larger than the peaks observed for α-olefins [62,63]. This indicates that in addition to oligomerizing ethylene, the catalyst system is undergoing extensive chainwalking followed by β-hydrogen elimination [9]. The chain walking is confirmed by the ^{13}C NMR of the polymer which indicates that the polymers are highly branched as 11.2 carbons per hundred are branch points. The majority, 61.9%, of these branch points result in methyl branching while ethyl, propyl and butyl and longer branches constitute 19.1%, 7.6% and 11.26% of the totals, respectively. The highly branched structure and relatively low molecular weight of the polymers are consistent with previous studies of nickel transition metal ethylene polymerization catalysts [64]. The ^{13}C NMR spectra of the same product reveals that the oligomer possesses a mixtures of branches, composed of methyl, ethyl and chains of four or more carbon atoms.

The production of oligomers led us to believe that the catalyst system would be particularly useful in the oligomerization of higher olefins to high molecular weight products. Indeed, when **4**/MAO was added to 1-decene in toluene the system produces waxy oligomers of 1-decene with molecular weights greater than 2000 g/mol. What was surprising was that these materials possess narrow PDIs of less than 1.1, indicating that the oligomerization of 1-decene proceeds without chain termination. At higher concentrations of MAO (Table 3, entry 4) the oligomerization produces materials of very low molecular weight (<500 g/mol) indicating that the MAO is either acting as a transfer agent, or at higher concentrations hinders the activity of the system. We suspect that the reduced PDI is due to the low number of insertions per metal site and the larger steric bulk of the olefin in comparison to ethylene.

3. Conclusions

In summary, the synthesis and characterization of two new nickel complexes was demonstrated. The reaction of *N*-(1-(3,5-dimethylpyrazol-1-yl)ethylidene)-2,6-diisopropylaniline or *N*-(1-(indazol-1-yl)ethylidene)-2,6-diisopropylaniline ligands and [$NiBr_2${($O(C_2H_4OMe)_2$}] gives **3** and **4**, respectively, in good yields. In the solid state, compound **4** exists as a dimer without an inversion center and unexpectedly exists in a *cis* ligand configuration. The reaction of **3** and **4** with 1000 equiv. of MAO yields ethylene polymerization sites. Under the same reaction conditions compound **4** has a higher polymerization activity, but due to the less crowded nickel center, this compound generates low molecular weight materials. In terms of polymers properties, the resulting materials are waxes with monomodal molecular weight distributions, consistent with the presence of a single active metal site. In addition, compound **4** was demonstrated to be efficient in the oligomerization of higher olefins to high molecular weights with narrow polydispersity.

4. Experimental

4.1. General remarks

All manipulations were performed under an inert atmosphere using standard glovebox and Schlenk-line techniques. All reagents were used as received from Aldrich unless otherwise specified. Ethylene was purchased from Matheson Tri-Gas (research grade, 99.99% pure) and was further purified by passage through an oxygen/moisture trap (Matheson model 6427-4S). Toluene, THF, hexane, and pentane were distilled from benzophenone ketyl. NEt_3 was dried over KOH. The starting compound *N*-(2,6-diisopropylphenyl)acetimidoylchloride was synthesized according to literature procedures [14]. $NiBr_2(O(C_2H_4OMe)_2$ was purchased from Aldrich and used as received. Polymerization reactions were carried out in a Parr autoclave reactor as described below. Toluene for polymerization was distilled from sodium/potassium alloy. NMR spectra were obtained using Varian Unity 200 and 400 Bruker spectrometers using deuterated solvent with TMS as internal standard. Polymers (waxes) were dried overnight under vacuum, and the polymerization activities were calculated from the mass of product obtained. These values were to within 5% of the calculated mass by measuring the ethylene consumed by use of a mass flow controller. The polymers were characterized by GPC analysis at 135 °C in o-dichlorobenzene (in a Polymer Laboratories, high-temperature chromatograph, Pl-GPC 200). ^{1}H NMR spectra of the polymers were obtained in solution (C_6D_6) at RT. Elemental analyses (C, H, N) were performed on a Fisons EA 1108 CHNS-O microanalyzer. Electron impact (EI) mass spectra were obtained at 70 eV on a Thermo-Finnigan MAT95 XP High Resolution Mass Spectrometer using perfluorokerosene (PFK) as reference. FTIR spectra were recorded on a Bruker Vector-22 spectrophotometer using KBr pellets. Melting point was determined using an Electrothermal melting point apparatus in open capillary tubes and are uncorrected.

4.2. Synthesis of ligands

4.2.1. *N*-(1-(3,5-dimethylpyrazol-1-yl)ethylidene)-2,6-diisopropylaniline (**1**)

A mixture of 3,5-dimethylpyrazole (0.89 g; 9.26 mmol), *N*-(2,6-diisopropylphenyl)acetimidoylchloride (2 g; 8.42 mmol) and NEt_3 (2 mL) in toluene (30 mL) was refluxed for 21 h with vigorous stirring. A white precipitate, Et_3NHCl, was formed and removed by filtration. The yellow solution was evaporated to dryness and gave a brown oil. This residue was dissolved in diethyl ether and purified by chromatography on Silica gel type 60. The compound was eluted with a mixture of dichloromethane-hexane (4:1) to give a brown oil. Yield 2.249 g (89%). NMR ($CDCl_3$, 295 K): ^{1}H, δ 7.14 (d, 2H, J_{HH} = 8 Hz, *m*-H-Ph), 7.07 (t, 1H, J_{HH} = 8 Hz, *p*-H-Ph), 6.05 (s, 1H, H (pirazole), 2.84 (hept, 2H, J_{HH} = 8 Hz, CH-*i*Pr), 2.66 (s, 3H, CH_3), 2.29 (s, 3H, CH_3-pirazole), 2.28 (s, 3H, CH_3-pirazole),

1.17 (d, 6H, J_{HH} = 8 Hz, CH_3-*i*Pr) and 1.13 (d, 6H, J_{HH} = 8 Hz, CH_3-*i*Pr) ppm. ^{13}C, δ 155.0, 149.0, 142.0, 123.53, 123.17, 123.08, 110.04, 22.25, 17.40, 15.82 and 13.73 ppm. IR (KBr, cm^{-1}): 1672 (s), 1573 (w), 1461 (w), 1438 (w), 1412 (m), 1385 (s), 1354 (s), 1326 (m), 1246 (w), 1087 (m), 966 (m), 775 (m), 755 (m). Anal. Calc. for $C_{19}H_{27}N_3$: C, 76.72; H, 14.15; N, 9.15. Found: C, 76.00; H, 13.93; N, 10.07%.

4.2.2. N-(1-(indazol-1-yl)ethylidene)-2,6-diisopropylaniline (**2**)

A suspension of indazole (1.094 g; 9.26 mmol), *N*-(2,6-diisopropylphenyl)acetimidoylchloride (2 g; 8.42 mmol) and NEt_3 (2 mL) in toluene (30 mL) was refluxed for 21 h with vigorous stirring. The white precipitate Et_3NHCl formed was removed by filtration and the yellow solution evaporated to dryness to give a white solid residue. The desired compound was isolated as white crystals from methanol. Yield 1.73 g (64.3%). M.p.: 112–114 °C. NMR ($CDCl_3$, 295 K): ^1H, δ 9.07 (s, 1H, H–C=N (indazole)), 7.71 (t, 2H, J_{HH} = 8 Hz, CH–CH (indazole)), 7.33 (t, 1H, J_{HH} = 8 Hz, *p*-H-Ph ($ArNH_2$)), 7.1–7.2 (m, 4H, H–C–C=N (indazole), H–C–N (indazole), 2*m*-H-Ph ($ArNH_2$)), 2.82 (hept, 2H, J_{HH} = 8 Hz, CH-*i*Pr), 2.48 (s, 3H, CH_3), 1.16 (d, 6H, J_{HH} = 8 Hz, CH_3-*i*Pr), and 1.14 (d, 6H, J_{HH} = 8 Hz, CH_3-*i*Pr) ppm. ^{13}C, δ 150.0, 142.91, 124.0, 123.4, 123.31, 122.0, 121.0, 120.0, 118.0, 23.27, 22.91 and 16.28 ppm. IR (KBr, cm^{-1}): 1673 (s), 1630 (w), 1520 (m), 1467 (m), 1406 (m), 1385 (s), 1334 (m), 1216 (s), 1147 (w), 1072 (w), 950 (w), 812 (m), 760 (s), 698 (m). Anal. Calc. for $C_{21}H_{25}N_3$: C, 78.96; H, 13.15; N, 7.89. Found: C, 78.97; H, 13.20; N, 7.83%.

4.3. Synthesis of complexes

4.3.1. [$NiBr_2${N-(1-(3,5-dimethylpyrazol-1-yl)ethylidene)-2,6-diisopropylaniline-N,N}] (**3**)

To a solution of [$NiBr_2\{O(C_2H_4OMe)_2\}$] (0.050 g; 0.142 mmol) in THF (15 mL), ligand **1** (0.042 g; 0.142 mmol) was slowly added. The solution was stirred at room temperature for 2 h. During this time the color of the solution changes slowly from orange to red. The solution was filtered through Celite and the solvent removed under vacuum to give an orange solid. The solid residue was washed two times with diethyl ether to afford a violet solid that was crystallized from dichloromethane-diethyl ether. Yield 0.066 g (90%). IR (KBr, cm^{-1}): 1633 (s), 1578 (s), 1460 (m), 1392 (s), 1364 (s), 1330 (s), 1196 (m), 1115 (m), 1052 (m), 1007 (m), 788 (m). EI-MS(+): m/z = 355.09 (M^+−2Br). Anal. Calc. for $C_{19}H_{27}Br_2N_3Ni$: C, 44.23; H, 5.27; N, 8.14. Found: C, 45.01; H, 5.67; N, 7.97%.

4.3.2. [$Ni_2Br_2(\mu$-Br)$_2${N-(1-(indazol-1-yl)ethylidene)-2,6-diisopropylaniline-N,N}$_2$] (**4**)

To a solution of $NiBr_2\{O(C_2H_4OMe)_2\}$ (0.050 g; 0.142 mmol) in dichloromethane (15 mL), ligand **2** (0.042 g; 0.142 mmol) was slowly added. The resulting orange solution was stirred at room temperature for 2 h then filtered through Celite. The solution was evaporated to dryness and the residue washed several times with diethyl ether to afford an orange solid. The complex was crystallized from a mixture of diethyl ether–pentane. Yield 0.061 g (80%). IR (KBr, cm^{-1}): 1628 (s, br), 1526 (s), 1468 (s), 1384 (m), 1366 (m), 1317 (s), 1224 (m), 1184 (w), 1134 (w), 1094 (s), 1008 (m), 974 (m), 825 (w), 800 (m), 760 (s). Anal. Calc. for $C_{42}H_{50}Br_4N_6Ni_2$: C, 46.74; H, 5.00; N, 7.77. Found: C, 46.89; H, 4.68; N, 7.81%.

4.4. X-ray crystallography

Crystals suitable for X-ray structure determination were obtained from a slow diffusion of pentane into a solution of complex **3** in toluene and from a mixture diethyl ether–pentane for complex **4**. The single crystals were mounted on a glass fiber and transferred to a Bruker CCD platform diffractometer. The SMART [65] program package was used to determine the unit-cell parameters and for data collection (25 s/frame scan time for a sphere of diffraction data). The raw frame data was processed using SAINT [66] and SADABS [67] to yield the reflection data file. Subsequent calculations were carried out using the SHELXTL [68] program. The structure was solved by direct methods and refined on F^2 by full-matrix least-squares techniques. The analytical scattering factors [69] for neutral atoms were used throughout the analysis. Hydrogen atoms were located from a difference Fourier map and refined (x, y, z and U_{iso}) [70]. The crystal data and refinement are summarized in Table 4.

Table 4
Crystal data and structure refinement for complexes **3** and **4**.

	3	**4**
Empirical formula	$C_{19}H_{27}N_3Br_2Ni$	$C_{42}H_{50}N_6Br_4Ni_2$
Formula weight	515.97	1075.94
Temperature (K)	150 (2)	150(2)
Wavelength (Å)	0.71073	0.71073
Crystal system	Monoclinic	Tetragonal
Space group	*P*2(1)/*n*	*P*4(3)2(1)2
Unit cell dimensions		
a (Å)	9.7927(3)	14.811(3)
b (Å)	17.0553(5)	14.811(3)
c (Å)	13.0366(4)	21.296(4)
α (°)	90	90
β (°)	93.0730(10)	90
γ (°)	90	90
Volume ($Å^3$)	2174.21(11)	4671.5(11)
Z	4	8
D_{calc} (Mg/m^3)	1.576	1.530
Absorption coefficient (mm^{-1})	4.574	4.262
F(000)	1040	2160
Crystal size (mm^3)	0.35 × 0.22 × 0.14	0.2 × 0.2 × 0.15
θ Range (°)	1.97–27.80	1.67–26.92
Index ranges	$-12 \leqslant h \leqslant 12$ $-21 \leqslant k \leqslant 21$ $-17 \leqslant l \leqslant 17$	$-18 \leqslant h \leqslant 16$ $-18 \leqslant k \leqslant 18$ $-26 \leqslant l \leqslant 26$
Reflections collected	29226	36920
Independent reflections	4862 [R_{int} = 0.0246]	4874 [R_{int} = 0.1481]
Completeness to θ = 26.48° (%) (for **1**) and 28.52° (%) (for **1′**, **2**)	99.8	97.2
Data/restraints/parameters	4862/0/233	4874/0/255
Goodness-of-fit on F^2	1.068	1.090
Final *R* indices [$I > 2\sigma(I)$]	R_1 = 0.0281, wR_2 = 0.0672	R_1 = 0.0540, wR_2 = 0.1272
R indices (all data)	R_1 = 0.0359, wR_2 = 0.0708	R_1 = 0.1571, wR_2 = 0.1532
Largest difference peak and hole (e $Å^{-3}$)	0.872 and −0.474	1.510 and −0.573

Definitions: $R_1 = \Sigma||F_o| - |F_c||/\Sigma|F_o|$, $wR_2 = [\Sigma(F_o^2 - F_c^2)^2]/\Sigma[w(F_o^2)^2]]^{1/2}$, GOF = $[\Sigma[w(F_o^2 - F_c^2)^2]/(n - p)]^{1/2}$, where n is the number of the reflections and p is the total number of the parameters refined. *Min/max.

Acknowledgments

The work was funded by FONDECYT Grant Nos. 11060384 and 1060597 and FONDAP Grant No. 11980002.

Appendix A. Supplementary material

Supplementary data associated with this article can be found, in the online version, at doi:10.1016/j.jorganchem.2009.01.005.

References

[1] H.H. Brintzinger, D. Fischer, R. Mülhaupt, B. Rieger, R.M. Waymouth, Angew. Chem., Int. Ed. Engl. 34 (1995) 1143.

[2] W. Kaminsky, H. Sinn (Eds.), Transition Metals and Organometallics as Catalysts for Olefin Polymerization, Springer-Verlag, Berlin, 1988.
[3] G. Fink, R. Mülhaupt, H.H. Brintzinger (Eds.), Ziegler Catalysts, Springer-Verlag, Berlin, 1995.
[4] A. Togni, R.L. Halterman (Eds.), Metallocenes, Wiley-VCH, New York, 1998.
[5] G.J.P. Britovsek, V.C. Gibson, D.F. Wass, Angew. Chem., Int. Ed. Engl. 38 (1999) 429.
[6] M.J. Bochmann, Chem. Soc., Dalton Trans. 3 (1996) 255.
[7] D. Rotman, Chem. Week 158 (1996) 37.
[8] M.M. Paige, Chem. Eng. News 76 (1998) 25.
[9] S.D. Ittel, L.K. Johnson, M. Brookhart, Chem. Rev. 100 (2000) 1169.
[10] .S. Mecking, Coord. Chem. Rev. 203 (2000) 325.
[11] V.C. Gibson, S.K. Spitzmesser, Chem. Rev. 103 (2003) 283.
[12] P. Galli, G. Vecellio, J. Polym. Sci. Part A: Polym. Chem. 42 (2004) 396.
[13] B. Rieger, L. Baugh, S. Striegler, S. Kacker, Late Transition Metal Polymerization Catalysis, John Wiley & Sons, New York, 2003.
[14] E. Anna, J.M. Rose, E.B. Lobkovsky, G.W. Coates, J. Am. Chem. Soc. 127 (2005) 13770.
[15] F. Auriemma, C. De Rosa, S. Esposito, G.W. Coates, M. Fujita, Macromolecules 38 (2005) 7416.
[16] J. Ruokolainen, R. Mezzenga, G.H. Fredrickson, E.J. Kramer, P.D. Hustad, G.W. Coates, Macromolecules 38 (2005) 851.
[17] A.F. Mason, G.W. Coates, J. Am. Chem. Soc. 126 (2004) 16326.
[18] A.F. Mason, G.W. Coates, J. Am. Chem. Soc. 126 (2004) 10798.
[19] M. Mitani, R. Furuyama, J.-I. Mohri, J. Saito, S. Ishii, H. Terao, T. Nakano, H. Tanaka, T. Fujita, J. Am. Chem. Soc. 125 (2003) 4293.
[20] E.F. Connor, T.R. Younkin, J.I. Henderson, S. Hwang, R.H. Grubbs, W.P. Roberts, J.J. Litzau, J. Polym. Sci. Part A: Polym. Chem. 40 (2002) 2842.
[21] G.M. Benedikt, E. Elce, B.L. Goodall, H.A. Kalamarides, L.H. McIntosh III, L.F. Rhodes, K.T. Selvy, C. Andes, K. Oyler, A. Sen, Macromolecules 35 (2002) 8978.
[22] A.C. Gottfried, M. Brookhart, Macromolecules 36 (2003) 3085.
[23] T.C. Chung, Prog. Polym. Sci. 27 (2002) 39.
[24] J.P. Matthew, A. Reinmuth, N. Swords, W. Risser, Macromolecules 29 (1996) 2755.
[25] B.L. Goodall, L.H. McIntosh, L.F. Rhodes, Macromol. Symp. 89 (1995) 421.
[26] S.C. Hong, S. Jia, M. Teodorescu, T. Kowalewski, K. Matyjaszewski, A.C. Gottfried, M. Brookhart, J. Polym. Sci. Part A: Polym. Chem. 40 (2002) 2736.
[27] A.M. Lapointe, A. Guram, T.S. Powers, B. Jandeleit, T.R. Boussie, C. Lund, WO 9946271, A1 990916, (1999), to Symyx Technologies.
[28] Y. Chauvin, H. Olivier, in: B. Cornils, W.A. Herrmann (Eds.), Applied Homogeneous Catalysis with Organometallic Compounds, vol. 1, VCH, Weinheim, Germany, 1996, pp. 258–268.
[29] B.L. Small, Organometallics 22 (2003) 3178.
[30] J.N.L. Dennett, A.L. Gillon, K. Heslop, D.J. Hyett, J.S. Fleming, C.E. Lloyd-Jones, A.G. Orpen, P.G. Pringle, D.F. Wass, J.N. Scutt, R.H. Weatherhead, Organometallics 23 (2004) 6077.
[31] F. Speiser, P. Braunstein, L. Saussine, Acc. Chem. Res. 38 (2005) 784.
[32] I. Albers, E. Alvarez, J. Campora, C.M. Maya, P. Palma, L.J. Sanchez, E.J. Passaglia, Organomet. Chem. 689 (2004) 833.
[33] F. Speiser, P. Braunstein, L. Saussine, R. Welter, Organometallics 23 (2004) 2613.
[34] W.-H. Sun, X. Tang, T. Gao, B. Wu, W. Zhang, H. Ma, Organometallics 23 (2004) 5037.
[35] Y. Chen, G. Wu, G.C. Bazan, Angew. Chem., Int. Ed. 44 (2005) 1108.
[36] Q.-Z. Yang, A. Kermagoret, M. Agostinho, O. Siri, P. Braunstein, Organometallics 25 (2006) 5518.
[37] T.R. Younkin, E.F. Connor, J.I. Henderson, S.K. Friedrich, R.H. Grubbs, D.A. Bansleben, Science 287 (2000) 460.
[38] R.S. Rojas, J.C. Wasilke, G. Wu, J.W. Ziller, G.C. Bazan, Organometallics 24 (2005) 5644.
[39] R.S. Rojas, G. Barrera Galland, G. Wu, G.C. Bazan, Organometallics 26 (2007) 5339.
[40] E.Y.-X. Chen, T.J. Marks, Chem. Rev. 100 (2000) 1391.
[41] S. Beck, S. Lieber, F. Schaper, A. Geyer, H.-H. Brintzinger, J. Am. Chem. Soc. 123 (2001) 1483.
[42] M.C. Bonnet, F. Dahan, A. Ecke, W. Keim, R.P. Schultz, I.J. Tkatchenko, J. Chem. Soc., Chem. Commun. (1994) 615.
[43] Z.J.A. Komon, X. Bu, G.C. Bazan, J. Am. Chem. Soc. 122 (2000) 1237.
[44] B.Y. Lee, G.C. Bazan, J. Vela, Z.J.A. Komon, X. Bu, J. Am. Chem. Soc. 123 (2001) 5352.
[45] C.B. Shim, Y.H. Kim, B.Y. Lee, Y. Dong, H. Yun, Organometallics 22 (2003) 4272.
[46] Y. Chen, B.M. Boardman, G. Wu, G.C. Bazan, J. Organomet. Chem. 692 (2007) 4745.
[47] G.J. Pindado, M. Thorton-Pett, M. Bouwkamp, A. Meetsma, B. Hessen, M. Bochmann, Angew. Chem., Int. Ed. Engl. 36 (1997) 2358.
[48] B. Temme, G. Erker, J. Karl, H. Luftman, R. Frohlich, S. Kotila, Angew. Chem., Int. Ed. Engl. 34 (1995) 1755.
[49] T.J. Marks, Acc. Chem. Res. 25 (1992) 57.
[50] X. Yang, C.L. Stern, T.J. Marks, J. Am. Chem. Soc. 116 (1994) 10015.
[51] S.L. Scott, B.C. Peoples, C. Yung, R.S. Rojas, V. Khanna, H. Sano, T. Suzuki, F. Shimizu, Chem. Commun. (2008) 4186.
[52] Z.J.A. Komon, G.M. Diamond, M.K. Leclerc, V. Murphy, M. Okazaki, G.C. Bazan, J. Am. Chem. Soc. 124 (2002) 15280.
[53] D.J. Parks, W.E. Piers, M. Parvez, R. Atencio, M.J. Zaworotko, Organometallics 17 (1998) 1369.
[54] Z.J.A. Komon, X. Bu, G.C. Bazan, J. Am. Chem. Soc. 122 (2000) 1830.
[55] Z.J.A. Komon, G.C. Bazan, Macromol. Rapid Commun. 22 (2001) 467.
[56] J.C. Wasilke, S.J. Obrey, R.T. Baker, G.C. Bazan, Chem. Rev. 105 (2005) 1001.
[57] B.M. Boardman, J.M. Valderrama, F. Muñoz, G. Wu, G.C. Bazan, R. Rojas, Organometallics 27 (2008) 1671.
[58] B. Rieger, L. Baugh, S. Striegler, S. Kacker, Late Transition Metal Polymerization Catalysis, John Wiley & Sons, New York, 2003 (Chapter 3).
[59] Y. Wang, S. Lin, F. Zhu, H. Gao, Q. Wu, Eur. Polym. J. (2008) 2308.
[60] R.T. Boeré, V. Klassen, G. Wolmershäuser, J. Chem. Soc., Dalton Trans. (1998) 4147.
[61] G. Luo, L. Chen, G. Dubowchik, J. Org. Chem. 71 (2006) 5392.
[62] G.B. Galland, R. Quijada, R. Rojas, G. Bazan, Z.J.A. Komon, Macromolecules 35 (2002) 339.
[63] P.M. Cotts, Z. Guan, E. McCord, S. McLain, Macromolecules 33 (2000) 6945.
[64] J.M. Rose, A.E. Cherian, G.W. Coates, J. Am. Chem. Soc. 128 (2006) 4186.
[65] SMART Software Users Guide, Version 5.1, Bruker Analytical X-ray Systems, Inc., Madison, WI, 1999.
[66] SAINT Software Users Guide, Version 6.0, Bruker Analytical X-ray Systems, Inc., Madison, WI, 1999.
[67] G.M. Sheldrick, SADABS, Version 2.05, Bruker Analytical X-ray Systems, Inc., Madison, WI, 2001.
[68] G.M. Sheldrick, SHELXTL, Version 6.12, Bruker Analytical X-ray Systems, Inc., Madison, WI, 2001.
[69] A.J.C. Wilson (Ed.), International Tables for X-ray Crystallography, vol. C, Kluwer Academic, Dordrecht, 1992.
[70] H.D. Flack, Acta Crystallogr. A39 (1983) 876.